Salicylketoximes targeting glucose transporter 1 restrict energy supply to lung cancer cells

Carlotta Granchi,[a] Yanrong Qian,[b] Hyang Yeon Lee,[c] Ilaria Paterni,[a] Carolina Pasero,[a] Jessica Iegre,[a] Kathryn E. Carlson,[c] Tiziano Tuccinardi,[a] Xiaozhuo Chen,[b] John A. Katzenellenbogen,[c] Paul J. Hergenrother,[c] and Filippo Minutolo*[,a]

Abstract: The glucose transporter GLUT1 is very frequently overexpressed in most tumor tissues because rapidly proliferating cancer cells rely mostly on glycolysis, a low-efficiency metabolic pathway necessitating a very high glucose consumption. Blocking GLUT1 is a promising anticancer strategy, thus we developed a novel class of GLUT1-inhibitors based on the 4-aryl-substituted salicylketoxime scaffold. Some of these compounds are efficient inhibitors of glucose uptake in lung cancer cells and have a noteworthy antiproliferative effect. In contrast to their 5-aryl-substituted regioisomers, the newly synthesized compounds reported herein do not display any significant binding to the estrogen receptors. The inhibition of glucose uptake in cancer cells by these compounds was further observed by fluorescence microscopy imaging using a fluorescent analog of glucose. Therefore, blocking the ability of tumor cells to take up glucose by means of these small-molecules, or by further optimized derivatives, may represent a successful approach in the development of novel anticancer drugs.

Introduction

The consumption of glucose in cancer cells is considerably higher than that of most normal cells, due to a metabolic shift that offers bioenergetic and biosynthetic advantages to cancer cells allowing non-oxidative ATP production to produce metabolic intermediates from glucose that are required to support the rapid proliferation of cancer cells.[1] This process is known as the "Warburg effect",[2] and is considered a strategic target to selectively hit cancer cells.[3] In fact, there is an increasing interest in considering glycolytic effectors as appropriate candidate targets for cancer therapy, and several antiglycolytic agents are currently being investigated for the treatment of cancer.[4] Overexpression of glucose transporters, in particular of glucose transporter 1 (GLUT1), has been found in several types of cancer cells, since they require enhanced glucose supply to support the less efficient energy production through anaerobic glycolysis; this elevated rate of glucose uptake has been widely exploited in the clinic for diagnostic imaging of tumors by positron emission tomography (PET) using 2-[^{18}F]fluoro-2-deoxyglucose (FDG).[5] Furthermore, the conjugation of anticancer agents to glucose or to its analogues that may potentially be recognized by GLUT1 offers the possibility to selectively target cancer cells with cytotoxic drugs.[6] Hence, there is a growing interest in GLUT1 as a potential target to effectively block cancer progression, although so far only a restricted number of GLUT1-inhibitors have been disclosed. A few years ago we identified some efficient GLUT1 inhibitors among a series of oxime derivatives,[7] and we constructed a GLUT1 model on the basis of the X-ray structure of XylE, an *Escherichia coli* homologue of GLUT1,[8] which was used to predict the binding poses and the most significant interactions that these compounds establish with GLUT1. More recently, a human GLUT1 crystal structure was obtained.[9]

To explore this synthetically accessible chemical class to find more potent and efficacious compounds and to further investigate their mechanism of action, we had to consider that this type of oxime is frequently found to bind efficiently to the estrogen receptors (ERs).[10] However, this is generally true only in the case of salicylaldoximes[11] and 5-aryl-substituted salicylketoximes,[12] whereas 4-aryl-substituted salicylketoximes show hardly any binding the ERs[11d] (Figure 1).

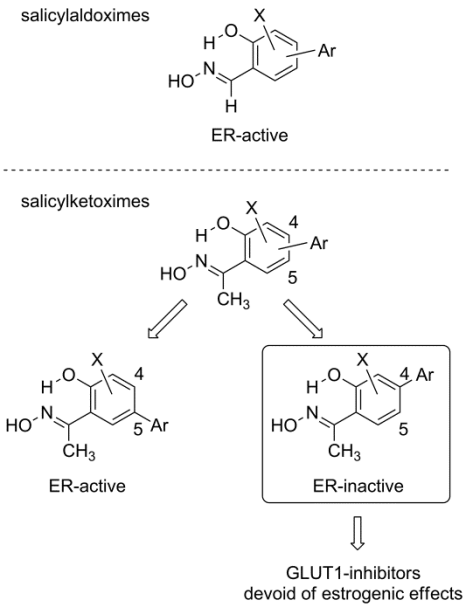

Figure 1. Selection of the chemical class of 4-aryl-substituted salicylketoximes as potential GLUT1-inhibitors devoid of binding affinities for the estrogen receptors.

[a] Dr. C. Granchi, I. Paterni, C. Pasero, J. Iegre, Prof. Dr. T. Tuccinardi, Prof. Dr. F. Minutolo
Dipartimento di Farmacia
Università di Pisa
Via Bonanno 33, 56126 Pisa, Italy
E-mail: filippo.minutolo@farm.unipi.it
[b] Dr. Y. Qian, Prof. Dr. X. Chen
Edison Biotechnology Institute
Ohio University, the Ridges
Athens, OH 45701, USA
[c] Dr. H.Y. Lee, K.E. Carlson, Prof. Dr. J.A. Katzenellenbogen, Prof. Dr. P.J. Hergenrother
Department of Chemistry
University of Illinois
600 S. Mathews Avenue, Urbana, IL 61801, USA

Supporting information for this article is given via a link at the end of the document: HPLC chromatograms, MS spectra, analytical data.

Therefore, to limit any possible side-activities on the ERs, this latter class of salicylketoximes was examined by inserting variously substituted aryl rings in position 4 (**3a-o**, Chart 1), and their GLUT1-inhibitory potencies were compared to that of two reference GLUT1-inhibitors (phloretin (**1**) and WZB117 (**2**)). Compounds **3a** and **3b** had already proved to possess promising GLUT1-inhibitory properties.[7] Therefore we retained their ketoxime portion and modified their 4-aryl substituents to extended this chemical class, producing ketoximes **3c**-**o**, some of which proved to efficiently block glucose uptake in cancer cells without interfering with the ERs.

Chart 1. Structures of reference GLUT1-inhibitors **1-2** and 4-aryl-substituted salicylketoximes **3a-o**.

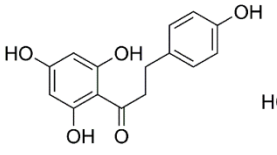

phloretin (**1**)

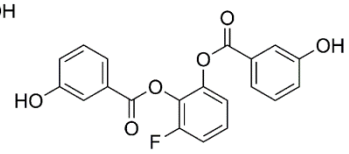

WZB117 (**2**)

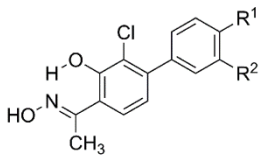

3a-o

a : $R^1 = OCH_3$; R^2 = F.
b : R^1 = OH; R^2 = H.
c : R^1 = F; R^2 = H.
d : $R^1 = CF_3$; R^2 = H.
e : R^1 = H; R^2 = OH.
f : R^1 = OH; R^2 = Cl.
g : $R^1 = OCF_3$; R^2 = H.
h : $R^1 = OCH_3$; R^2 = H.
i : R^1 = H; $R^2 = OCF_3$.
j : R^1 = H; $R^2 = OCH_3$.
k : R^1 = CN; R^2 = H.
l : R^1 = H; R^2 = CN.
m : $R^1 = OCH_3$; R^2 = Cl.
n : $R^1 = OCH_3$; $R^2 = CH_3$.
o : R^1 = OH; $R^2 = CH_3$.

Results and Discussion

Chemistry. Compounds **3a** and **3b** were synthesized as previously described,[11d] whereas the synthesis of **3c**-**o** followed a common synthetic pathway (Scheme 1) starting from 4-bromo-3-chloro-2-hydroxyacetophenone **4**.[11d] Biaryl compounds **5c-o** were obtained by a Pd-catalyzed cross-coupling reaction of **4** with the properly substituted arylboronic acids. Classical Suzuki conditions, including the use of an aqueous sodium carbonate solution as the base, were suitable for most of these derivatives (**5c-j** and **5m-o**). However, the synthesis of cyano-substituted intermediates **5k** and **5l** required anhydrous conditions to prevent the undesired hydrolysis of the cyano group under prolonged heating in the presence of alkaline solutions. Therefore, in these cases, we used anhydrous potassium carbonate as the base in the cross-coupling step, and we removed ethanol from the solvent system; finally, the amount of boronic acid was increased from 1.3 to 2 equivalents. These conditions allowed us to produce **5k** and **5l** efficiently. Hydroxy-substituted intermediates **5e**, **5f** and **5o**, were respectively obtained by treatment of methoxy-substituted biaryl ketones **5j**, **5m** and **5n**, with BBr_3. All the resulting acetophenone derivatives **5c**-**o** were directly transformed into the corresponding salicylketoximes **3c-o** by reaction with hydroxylamine hydrochloride.

Scheme 1. Synthesis of salicylketoximes **3c-o**.[a]

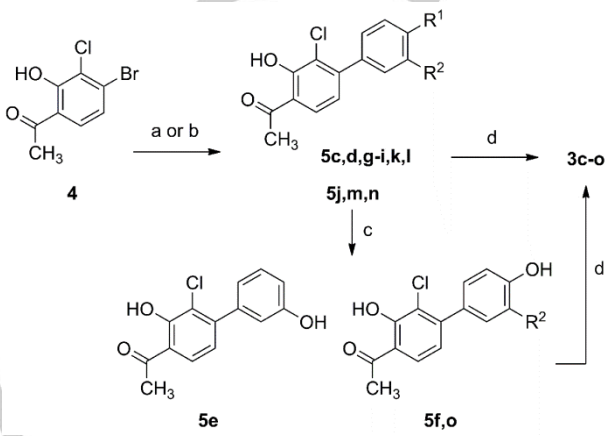

[a] Reagents and conditions: (a) $ArB(OH)_2$ (1.3 eq), $Pd(OAc)_2$ (0.02 eq), PPh_3 (0.1 eq), aqueous 2M Na_2CO_3, 1:1 toluene/EtOH, 100 °C, 16 h; (b) $ArB(OH)_2$ (2 eq), $Pd(OAc)_2$ (0.03 eq), PPh_3 (0.15 eq), solid K_2CO_3 (1.5 eq), toluene, 100 °C, 24 h; (c) BBr_3, CH_2Cl_2, –78 to 0 °C, 1 h; (d) $NH_2OH{\cdot}HCl$, EtOH-H_2O, 50 °C, 16 h.

As we previously observed for 5-aryl-substituted salicylketoxime derivatives,[12] these 4-aryl-substituted ketoximes **3c**-**o** were exclusively obtained as diastereoisomers of *E*-configuration in their oxime portion. This is due to the stabilization induced by the highly energetic intramolecular H-bond between the phenolic OH group and the nearby nitrogen atom of the oxime portion. Spectroscopic evidence supporting these configurations was obtained by ^{1}H- and ^{13}C-NMR analysis. In fact, the ^{1}H-NMR chemical shift values (δ) of the ketoximic methyl protons ($2.40 \leq \delta \leq 2.43$ ppm) and the ^{13}C-NMR δ values of the ketoximic methyl carbon atom ($10.91 \leq \delta \leq 10.96$ ppm), strictly parallel those reported in the literature for the *E*-isomers of similar methyl-ketoxime derivatives.[12]

Biological evaluation. The newly synthesized compounds (**3c**-**o**) were screened for inhibition of glucose transport through GLUT1 by means of a standard glucose uptake assay, as previously described. [7,13] This method consists of the treatment of H1299 human non-small cell lung carcinoma (NSCLC) cells with a 30 µM concentration of the compounds for 15 min. Then, these cells were incubated in the glucose-free KRP buffer with 2-deoxy-D-[^{3}H]-glucose for 30 min. After washing the cells with cold PBS, they were lysed in 0.2 M NaOH, and the lysates were transferred to scintillation counting vials. The radioactivity in the cell lysates was finally quantified by liquid scintillation counting and the results are listed in Table 1 as % uptake of control samples. The compounds that gave the highest inhibition (<

20% Glc uptake) at the 30 μM concentration (**3e,f,o**), were further studied at various concentrations to produce dose-response curves, which were used for the determination of their IC_{50} values. These values could be then compared to those of reference GLUT1-inhibitors such as phloretin (**1**) and WZB117 (**2**), together with those of previously reported ketoximes **3a** and **3b**. It is interesting to note that compound **3e** is a close analogue of **3b**, where the phenolic *para*-hydroxy group is shifted to the *meta*-position, whereas **3f** and **3o** derive from insertion of a *meta*-chloro or *meta*-methyl substituent, respectively, into the structure of **3b**. The data so obtained (Table 1) show that newly synthesized compounds **3e** and **3o** have IC_{50} values (15.7 and 11.1 μM, respectively) comparable to those of reference GLUT1-inhibitors, with the exception of **3f**, which displayed the highest potency of this series (IC_{50} = 7.0 μM). It is worth noting that the replacement of the phenolic *para*-OH group of **3b** with a fluorine atom (**3c**), CF_3 (**3d**), OCF_3 (**3g**), OCH_3 (**3h,m,n**) or CN (**3k**) groups, caused a significant drop of activity. A similar effect was observed when the phenolic *meta*-OH group of **3e** was replaced by OCF_3 (**3i**), OCH_3 (**3j**) or CN (**3l**) groups. An SAR analysis of these results obtained with newly synthesized compounds **3c**-**o** highlights the fundamental role played by the phenolic OH group present in either the *para*- (**3e**, **3o**) or *meta*- (**3f**) positions of the 4-aryl substituent.

Table 1. Inhibitory activities on glucose uptake and cell growth (H1299) of compounds **1**, **2**, **3a**-**o**, together with their estrogen receptor (ER) relative binding affinities (RBA, %).

Cpd	GLUT1[a]		H1299[a]		ER binding affinity (RBA, %)[b]	
	Glc uptake (%) at 30 μM	inhibition, IC_{50} (μM)	viability (%) at 30 μM	cytotoxicity, IC_{50} (μM)	ERα	ERβ
1	21 ± 9[c]	21.4 ± 5.1[c]	72 ± 10[c]	54.0 ± 14.6[c]	0.206[d]	-
2	16 ± 4[c]	10.9 ± 3.6[c]	35 ± 9[c]	20.4 ± 4.8[c]	-	-
3a	17 ± 3[c]	15.5 ± 3.8[c]	32 ± 4[c]	39.6 ± 11.8[c]	<0.001[e]	0.002 ± 0.001[e]
3b	9 ± 4[c]	10.6 ± 2.8[c]	42 ± 5[c]	34.8 ± 5.8[c]	0.012 ± 0.004[e]	0.123 ± 0.030[e]
3c	102 ± 4	-	69 ± 8	-	<0.001	<0.001
3d	100 ± 4	-	89 ± 8	-	0.003 ± 0.001	<0.001
3e	16 ± 1	15.7 ± 2.0	22 ± 8	17.8 ± 2.8	<0.001	0.003 ± 0.001
3f	9 ± 3	7.0 ± 2.0	80 ± 8	45.8 ± 7.4	0.008 ± 0.002	0.010 ± 0.002
3g	81 ± 3	-	106 ± 8	-	0.009 ± 0.002	0.037 ± 0.010
3h	85 ± 2	-	73 ± 8	-	0.007 ± 0.001	0.016 ± 0.001
3i	75 ± 5	-	83 ± 7	-	0.015 ± 0.001	0.028 ± 0.001
3j	67 ± 16	-	90 ± 6	-	0.009 ± 0.001	0.014 ± 0.003
3k	78 ± 7	-	75 ± 5	-	0.008 ± 0.001	0.027 ± 0.006
3l	67 ± 10	-	82 ± 9	-	0.013 ± 0.003	0.042 ± 0.006
3m	79 ± 5	-	65 ± 5	-	0.015 ± 0.003	0.034 ± 0.007
3n	78 ± 2	-	76 ± 2	-	0.020 ± 0.001	0.047 ± 0.006
3o	8 ± 1	11.1 ± 2.6	62 ± 8	30.3 ± 5.9	0.018 ± 0.004	0.034 ± 0.004

[a] These compounds were tested in a standard glucose uptake and cytotoxicity assays as previously described. Ref. [13]. [b] Determined by a competitive radiometric binding assay as previously described. Ref. [14]. Values are reported as the mean ± the range or SD of 3 or more independent experiments; the K_d of estradiol for ERα is 0.2 nM and for ERβ is 0.5 nM. K_i values for the new compounds can be readily calculated by using the formula: $K_i = (K_d[\text{estradiol}]/\text{RBA}) \times 100$. [c] Ref. [7]. [d] Rat uterine estrogen receptors (Ref. [15]). [e] Ref. [11d].

All the newly synthesized compounds were also subjected to an antiproliferative MTT assay in the same NSCLC H1299 cell line. In this case the cells were incubated for 48 h in presence of a 30 µM concentration of the compounds and the percentage values of viable cells are reported in Table 1. In this case the most potent GLUT1-inhibitors **3e** and **3o** also displayed the most potent cytotoxic properties among the newly synthesized ketoximes, whereas **3f** proved to be less cytotoxic than the other two compounds. Complete dose-response curves for compounds **3e,f,o**, indicate IC_{50} values of 17.8 (**3e**), 45.8 (**3f**), and 30.3 (**3o**) µM. Overall, we generally found a parallelism between GLUT1-inhibitory potency and anti-proliferative effect. Compound **3f** constitutes the most evident exception, since it displays the highest potency of the series as GLUT1 inhibitor, but a relatively low cytotoxicity. Therefore, we cannot exclude the concomitant involvement of other mechanisms in the inhibition of proliferation by this type of compounds.

In order to assess any possible interference with the estrogen receptors ERα and ERβ, all the newly synthesized compounds were subjected to a radiometric competitive binding assay, as previously reported.[14] The relative binding affinity (RBA) values so obtained, together with those previously reported for phloretin (**1**),[15] and ketoximes **3a,b**[11d] are indicated in Table 1. These values are reported as percentages (%) of that of estradiol, which is set at 100%. It should be noticed that reference GLUT1-inhibitor phloretin was reported to possess a RBA of 0.206% on ERα,[15] which corresponds to an absolute binding affinity (K_i) of about 0.1 µM. Ketoxime **3b** had already displayed a certain binding affinity for ERβ (RBA = 0.123%; K_i = 0.4 µM). We were pleased to find that all the newly synthesized ketoximes **3c**-**o** and, in particular, those showing the most promising GLUT1-inhibitory properties (**3e,f,o**), show only negligible binding affinities values for both ERs, thus confirming their selectivity for the GLUT transporter over the estrogen receptors. It should be noted that this selective activity is particularly useful from a therapeutic perspective since it avoids the possible intervention of estrogenic effects, although potential benefits from the simultaneous GLUT1-inhibition and ERβ-selective stimulation[10] might deserve further investigation for the development of anticancer drugs with a dual mechanism of action.

Encouraged by these results, we were then able to visualize the inhibition of glucose uptake in cancer cells by fluorescence microscopy, and to quantify the inhibitory potencies of this type of compounds. For this purpose, we used a fluorescent d-glucose analog, 2-[*N*-(7-nitrobenz-2-oxa-1,3-diazol-4-yl) amino]-2-deoxy-d-glucose (2-NBDG), which was reported to be a suitable probe for the detection of glucose taken up by cultured cells.[16] Briefly, A549 non-small lung carcinoma cells were treated in glucose free RPMI 1640 media for 30 minutes with 30 µM phloretin (**1**), as the reference GLUT1-inhibitor, or ketoximes **3a,e,f,o**, which are those among this chemical class that displayed the highest GLUT1-inhibitory properties and negligible ER binding affinities. Then the cells were sequentially treated with 2-NBDG (50 µM) and Hoechst 33342 (1 µg/mL) for 15 minutes. After 15 minutes, the cells were washed with a glucose-free RPMI 1640 medium. Accumulation of intracellular 2-NBDG, excited at 488 nm, was imaged using a confocal laser scanning microscope (LSM700) with 40x objective. The images so obtained are shown in Figure 2.

An evident reduction of 2-NBDG uptake by cancer cells, which is represented by a reduced green fluorescence of the cytosol compared to the nuclear blue stain, was observed after treatment with all the compounds used, when compared to DMSO control. Furthermore, ketoxime derivatives seem to produce stronger effects than that of phloretin. In order to quantify these effects, the mean fluorescence intensities of 100~120 cells were measured using Image J, and the average values of quadruplicate experiments are reported in Figure 3.

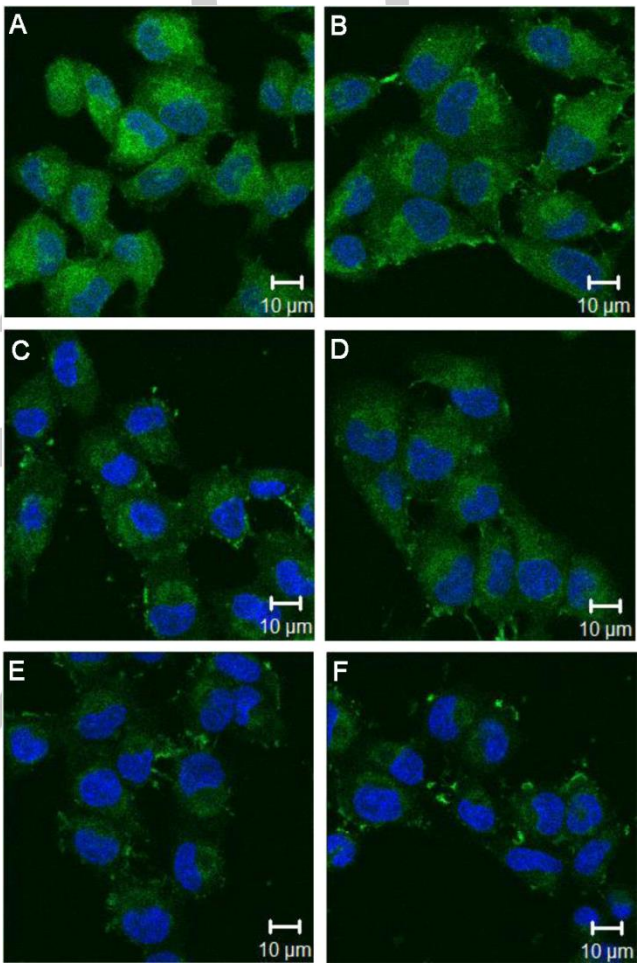

Figure 2. Fluorescence imaging of intracellular accumulation of 2-NBDG in A549 cancer cells upon treatment with selected GLUT1-inhibitors (30 µM): DMSO control (A), **1** (B), **3a** (C), **3e** (D), **3f** (E), **3o** (F). Scale bar indicates 10 µm.

This analysis further demonstrates that the ketoxime-based GLUT1-inhibitors show a more potent effect (33-49% residual fluorescence, Figure 3 and Table S1, supporting information) than that of phloretin (67%, Figure 3 and Table S1) in reducing the cellular uptake of 2-NBDG. Among these compounds, **3o** proved to be the most active inhibitor (33%, Table S1), followed by **3f** (38%, Table S1)

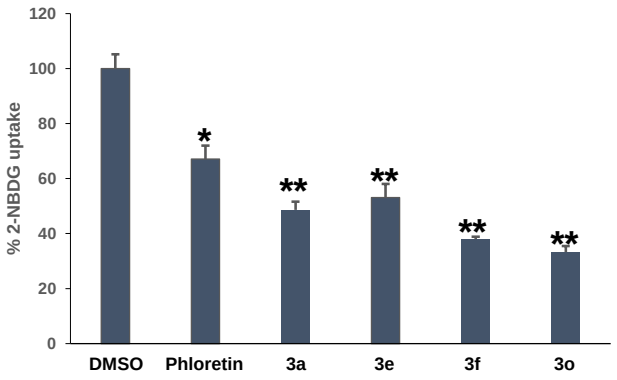

Figure 3. Quantitative measurement of cellular uptake of 2-NBDG by A549 cancer cells in the presence of selected GLUT1-inhibitors by measurement of fluorescence intensity. Error bars denote standard errors (n=4). Statistical analysis was performed using Student's unpaired, two-tailed t test; * $0.001 < p \leq 0.005$; ** $p \leq 0.001$ compared to vehicle (DMSO) treatment.

Molecular modeling and design. The three most promising GLUT1-inhibitors (**3e**, **3f** and **3o**) were docked, using GOLD[17] into our recently published *h*GLUT1 homology model.[7] All three compounds showed a very similar disposition, with the oxime hydroxy group forming an H-bond with the backbone C=O of residue Q397. The phenolic hydroxyl in position 2 showed two H-bonds with the backbone C=O of E146 and the backbone N-H of R212, respectively (see Figure 4). The ketoximic central scaffold showed a π-arginine stacking interaction with R212, whereas the chlorine atom present in the central scaffold was inserted into a pocket delimited by S148 and R232. The aryl substituent in position 4 of the central ring showed a lipophilic interaction with F460. Furthermore, the *p*-hydroxy groups of compound **3f** and **3o** participate to a network of H-bonds with the backbone N-H of F460 and the backbone C=O of P149. Differently, the *m*-hydroxyl group of compound **3e** forms a single H-bond (as a donor) with the anionic carboxylate present in the side chain of E243. This analysis confirms the importance of the para/meta-hydroxyaryl substituent in the interaction of the most potent inhibitors (**3e**, **3f**, and **3o**) with the transporter.

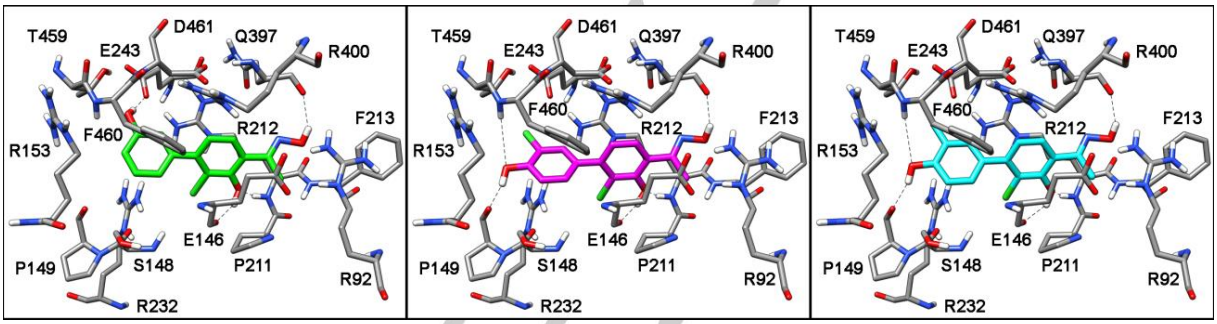

Figure 4. Docking analysis into the *h*GLUT1 model of **3e** (green), **3f** (magenta), and **3o** (sky blue).

Conclusions

In summary, we synthesized a selected series of 4-aryl-substituted salicyl-ketoximes, which were designed to selectively target the greatly elevated glucose dependence shown by tumors, and we investigated their activity as inhibitors of glucose transporter GLUT1 in lung cancer cells. The antiproliferative activity of these compounds was also assessed and compared to their ability to inhibit glucose uptake. A careful molecular design produced some compounds displaying selective interactions with GLUT1 and, at the same time, being devoid of cross-interference with the estrogen receptors (ERs), which often bind this type of oximes (5-aryl-substituted salicylketoximes) or other phenolic derivatives (see, for example, phloretin itself).

An important aspect of this work is that we were able to provide additional evidence for the inhibition of GLUT1 by means of the visualization of the uptake of a fluorescent analogue of glucose. A quantification of the intracellular fluorescence, which proved to be significantly reduced by administration of these compounds, further support their mechanism of action. Furthermore, a large set of molecules of this class may be easily prepared in 2-3 steps from common intermediate **4**, using cross-coupling reactions with various arylboronic acids, followed by a condensation with hydroxylamine. This easy synthetic accessibility should allow the preparation of larger collections to further explore this promising chemical class in the near future.

Experimental Section

General procedures and materials. All solvents and chemicals were used as purchased without further purification. Chromatographic separations were performed on silica gel columns by flash (Kieselgel 40, 0.040–0.063 mm; Merck) chromatography. Reactions were followed by thin-layer chromatography (TLC) on Merck aluminum silica gel (60 F_{254}) sheets that were visualized under a UV lamp. Evaporation was performed in vacuo (rotating evaporator). Sodium sulfate was always used as the drying agent. Proton (^{1}H) and carbon (^{13}C) NMR spectra

were obtained with a Bruker Avance III 400 MHz spectrometer using the indicated deuterated solvents. Chemical shifts are given in parts per million (ppm) (δ relative to residual solvent peak for ^{1}H and ^{13}C). Yields refer to isolated and purified products. LC-MS characterization and high-resolution mass spectrometry (HRMS) analysis were performed using a Waters Quattro II quadrupole-hexapole-quadrupole liquid chromatography/mass spectrometry apparatus (Waters, Milford, MA) equipped with an electrospray ionization source. Reverse phase HPLC (Shimadzu corporation, Japan) analysis was performed using a clarity 3µm oligo-RP C-18 column (150 x 4.6 mm, Phenomenex, US) at a flow rate of 0.5 mL/min at 25 °C. Each sample was dissolved in DMSO at a concentration of 100 mM and diluted to 10 µM in DMSO for HPLC analysis. HPLC solvents consist of water containing 0.1 % TFA and acetonitrile containing 0.1 % TFA. The elution protocol for analytical HPLC starts with 40% acetonitrile for 5min, followed by a linear gradient to 100% acetonitrile over 20 min and held at 100% acetonitrile for 10 min. The ultraviolet (UV) detector was programmed to monitor absorbance at 300 nm. Yields refer to isolated and purified products deriving from non-optimized procedures.

Preparation of ketones 5c, d, g-j, m, n. General procedure. A solution of $Pd(OAc)_2$ (0.02 eq) and triphenylphosphine (0.1 eq) in ethanol (1.7 mL/1.36 mmol compound **4**) and toluene (1.7 mL/1.36 mmol compound **4**) was stirred at RT under nitrogen for 10 min. After that period, compound **4** (1 eq), 1.7 mL of an aqueous 2 M solution of Na_2CO_3, and the properly substituted arylboronic acid (1.3 eq) were sequentially added. The resulting mixture was heated at 100 °C in a sealed vial under nitrogen overnight. After being cooled to RT, the mixture was diluted with water and extracted with EtOAc. The combined organic phase were dried and concentrated. The crude product was purified by flash chromatography by eluting with *n*-hexane/EtOAc (95:5 to 9:1) affording the desired ketone intermediates.

1-(2-Chloro-4'-fluoro-3-hydroxy-[1,1'-biphenyl]-4-yl)ethanone (5c). (81% yield from **4**) ^{1}H NMR (400 MHz, [D$_6$]acetone): δ=2.75 (s, 3H), 7.02 (d, J=8.3 Hz, 1H), 7.27 (double AA'XX', $^{3}J_{HF-o}$=9.8 Hz, J_{AX}=8.9 Hz, $J_{AA'XX'}$=2.2 Hz, 2H), 7.54 (double AA'XX', $^{4}J_{HF-m}$=5.4 Hz, J_{AX}=8.9 Hz, $J_{AA'XX'}$=2.5 Hz, 2H), 8.00 (d, *J*=8.3 Hz, 1H), 13.12 ppm (*exchangeable* s, 1H); ^{13}C NMR (100 MHz, [D$_6$]acetone): δ=27.0, 116.0 (d, *J*=22.1 Hz, 2C), 120.3, 121.3, 121.9, 130.4, 132.1 (d, *J*=9.1 Hz, 2C,), 135.7 (d, *J*=3.0 Hz), 147.7, 159.4, 163.6 (d, *J*=246.5 Hz), 170.9 ppm.

1-(2-Chloro-3-hydroxy-4'-(trifluoromethyl)-[1,1'-biphenyl]-4-yl)ethanone (5d). (62% yield from **4**) ^{1}H NMR (400 MHz, [D$_6$]acetone): δ=2.78 (s, 3H), 7.07 (d, *J*=8.2 Hz, 1H,), 7.70-7.74 (m, 2H), 7.84-7.88 (m, 2H), 8.06 (d, *J*=8.3 Hz, 1H), 13.12 ppm (*exchangeable* s, 1H); ^{13}C NMR (100 MHz, $CDCl_3$): δ=27.0, 119.7, 120.8, 121.6, 124.2 (q, *J*=272.7 Hz), 125.4 (q, *J*=4.0 Hz, 2C), 128.7, 129.7 (2C), 130.7 (q, *J*=33.2 Hz), 142.1, 146.8, 158.9, 204.2 ppm.

1-(2-Chloro-3-hydroxy-4'-(trifluoromethoxy)-[1,1'-biphenyl]-4-yl)ethanone (5g). (79% yield from **4**) ^{1}H NMR (400 MHz, [D$_6$]acetone): δ =2.76 (s, 3H), 7.05 (d, *J*=8.2 Hz, 1H), 7.44-7.49 (m, 2H), 7.63 (AA'XX', J_{AX}=8.9 Hz, $J_{AA'XX'}$=2.5 Hz, 2H), 8.03 (d, *J*=8.3 Hz, 1H), 13.11 ppm (*exchangeable* s, 1H); ^{13}C NMR (100 MHz, [D$_6$]acetone): δ=27.0, 120.6, 121.4 (q, *J*=255.6 Hz), 121.6 (2C), 121.8, 130.4, 131.9 (2C), 132.2, 133.9, 138.6, 147.3, 149.9, 159.3 ppm.

1-(2-Chloro-3-hydroxy-4'-methoxy-[1,1'-biphenyl]-4-yl)ethanone (5h). (69% yield from **4**) ^{1}H NMR (400 MHz, $CDCl_3$): δ=2.68 (s, 3H), 3.87 (s, 3H), 6.92 (d, *J*=8.3 Hz, 1H), 6.99 (AA'XX', J_{AX}=8.9 Hz, $J_{AA'XX'}$=2.5 Hz, 2H), 7.42 (AA'XX', J_{AX}=8.9 Hz, $J_{AA'XX'}$=2.5 Hz, 2H), 7.69 (d, *J*=8.3 Hz, 1H), 13.10 ppm (*exchangeable* s, 1H); ^{13}C NMR (100 MHz, $CDCl_3$): δ=26.8, 55.5, 113.8 (2C), 119.0, 121.2, 121.4, 128.4, 130.6 (2C), 130.9, 148.1, 158.9, 159.9, 204.1 ppm.

1-(2-Chloro-3-hydroxy-3'-(trifluoromethoxy)-[1,1'-biphenyl]-4-yl)ethanone (5i). (78% yield from **4**) ^{1}H NMR (400 MHz, [D$_6$]acetone): δ=2.77 (s, 3H), 7.07 (d, *J*=8.2 Hz, 1H), 7.43-7.47 (m, 2H), 7.52 (dt, *J*=8.0, 1.3 Hz, 1H), 7.66 (dd, *J*=8.9, 7.7 Hz, 1H), 8.04 (d, *J*=8.3 Hz, 1H), 13.12 ppm (*exchangeable* s, 1H); ^{13}C NMR (100 MHz, [D$_6$]acetone): δ=27.1, 120.7, 121.3, 121.5 (q, *J*=255.6 Hz), 121.8, 121.8, 122.7, 129.0, 130.6, 131.2, 141.6, 147.0, 149.7, 159.4, 170.9 ppm.

1-(2-Chloro-3-hydroxy-3'-methoxy-[1,1'-biphenyl]-4-yl)ethanone (5j). (97% yield from **4**) ^{1}H NMR (400 MHz, $CDCl_3$): δ=2.69 (s, 3H), 3.85 (s, 3H), 6.93 (d, *J*=8.3 Hz, 1H), 6.95-7.05 (m, 3H), 7.38 (t, *J*=7.9 Hz, 1H), 7.71 (d, *J*=8.3 Hz, 1H), 13.08 ppm (*exchangeable* s, 1H); ^{13}C NMR (100 MHz, $CDCl_3$): δ=26.9, 55.5, 114.1, 115.0, 119.3, 121.1, 121.6, 128.4, 129.4, 140.0, 148.3, 158.9, 159.5, 204.2 ppm.

1-(2,3'-Dichloro-3-hydroxy-4'-methoxy-[1,1'-biphenyl]-4-yl)ethanone (5m). (88% yield from **4**) ^{1}H NMR (400 MHz, $CDCl_3$): δ=2.68 (s, 3H), 3.96 (s, 3H), 6.90 (d, *J*=8.3 Hz, 1H), 7.01 (d, *J*=8.6 Hz, 1H), 7.37 (dd, *J*=8.5, 2.2 Hz, 1H), 7.49 (d, *J*=2.2 Hz, 1H), 7.70 (d, *J*=8.3 Hz, 1H), 13.08 ppm (*exchangeable* s, 1H); ^{13}C NMR (100 MHz, $CDCl_3$): δ=26.9, 56.4, 111.7, 119.3, 121.0, 121.6, 122.5, 128.5, 128.9, 131.1, 131.7, 146.7, 154.8, 159.0, 204.1 ppm.

1-(2-Chloro-3-hydroxy-4'-methoxy-3'-methyl-[1,1'-biphenyl]-4-yl)ethanone (5n). (94% yield from **4**) ^{1}H NMR (400 MHz, $CDCl_3$): δ=2.28 (s, 3H), 2.68 (s, 3H), 3.89 (s, 3H), 6.91 (d, *J*=8.4 Hz, 1H), 6.92 (d, *J*=8.3 Hz, 1H), 7.24-7.27 (m, 1H), 7.31 (dd, *J*=8.4, 2.2 Hz, 1H), 7.68 (d, *J*=8.3 Hz, 1H), 13.10 ppm (*exchangeable* s, 1H); ^{13}C NMR (100 MHz, $CDCl_3$): δ=16.4, 26.8, 55.5, 109.6, 118.9, 121.2, 121.4, 126.6, 128.0, 128.3, 130.5, 131.5, 148.4, 158.1, 158.9, 204.1 ppm.

Preparation of ketones 5k, l. General procedure. A solution of $Pd(OAc)_2$ (0.03 eq) and PPh_3 (0.15 eq) in toluene (3.1 mL) was stirred at RT under nitrogen for 10 min. Compound **4** (80 mg, 0.32 mmol), K_2CO_3 (1.5 eq) and 4-(cyano)phenylboronic acid or 3-(cyano)phenylboronic acid (2 eq) were sequentially added. The resulting mixture was heated at 100 °C in a sealed vial under nitrogen overnight. After being cooled to RT, the mixture was diluted with water and extracted with EtOAc. The crude product was purified with flash chromatography by eluting with *n*-hexane/EtOAc 8: 2 to afford cyano-substituted compounds.

4'-Acetyl-2'-chloro-3'-hydroxy-[1,1'-biphenyl]-4-carbonitrile (5k). (55% yield from **4**) ^{1}H NMR (400 MHz, $CDCl_3$): δ=2.71 (s, 3H), 6.89 (d, *J*=8.3 Hz, 1H), 7.56 (AA'XX', J_{AX}=8.6 Hz, $J_{AA'XX'}$=1.8 Hz, 2H), 7.74-7.78 (m, 3H), 13.08 ppm (*exchangeable* s, 1H); ^{13}C NMR (100 MHz, $CDCl_3$): δ=26.9, 112.5, 118.6, 119.9, 120.5, 128.7, 130.0 (2C), 132.2 (2C), 143.1, 146.1, 158.9, 174.5, 204.2 ppm.

4'-Acetyl-2'-chloro-3'-hydroxy-[1,1'-biphenyl]-3-carbonitrile (5l). (69% yield from **4**) ^{1}H NMR (400 MHz, $CDCl_3$): δ=2.71 (s, 3H), 6.89 (d, *J*=8.2 Hz, 1H), 7.58 (t, *J*=7.7 Hz, 1H), 7.68-7.74 (m, 3H), 7.76 (d, *J*=8.0 Hz, 1H), 13.09 ppm (*exchangeable* s, 1H); ^{13}C NMR (100 MHz, $CDCl_3$): δ=26.9, 112.8, 118.5, 119.6, 120.7, 121.6, 128.8, 129.3, 132.1, 132.8, 133.7, 139.8, 145.7, 158.9, 204.2 ppm.

Preparation of *O*-deprotected ketones 5e, f, o. General Procedure. A solution of pure ketones **5j, m, n** (0.50 mmol) in anhydrous CH_2Cl_2 (5.8 mL) was cooled to −78 °C and treated dropwise with a 1.0 M solution of BBr_3 in CH_2Cl_2 (1.5 mL) under nitrogen. The mixture was left under stirring at the same temperature for 5 min and then at 0 °C for 1 h. The

mixture was then diluted with water and extracted with EtOAc. The organic phase was dried and concentrated. The crude product was purified by flash chromatography over silica gel. Elution with *n*-hexane/EtOAc (8:2 to 7:3) afforded the desired *O*-deprotected ketones.

1-(2-chloro-3,3'-dihydroxy-[1,1'-biphenyl]-4-yl)ethanone (5e). (65% yield from **5j**) ^{1}H NMR (400 MHz, $CDCl_3$): δ=2.69 (s, 3H), 4.94 (*exchangeable* bs, 1H), 6.88-6.94 (m, 3H), 7.01 (dt, *J*=7.7, 1.3 Hz, 1H), 7.33 (t, *J*=7.8 Hz, 1H), 7.70 (d, *J*=8.3 Hz, 1H), 13.08 ppm (*exchangeable* s, 1H); ^{13}C NMR (100 MHz, $CDCl_3$): δ=26.9, 115.5, 116.2, 119.3, 121.0, 121.5, 121.8, 128.4, 129.7, 140.2, 147.9, 155.4, 158.8, 204.2 ppm.

1-(2,3'-Dichloro-3,4'-dihydroxy-[1,1'-biphenyl]-4-yl)ethanone (5f). (87% yield from **5m**) ^{1}H NMR (400 MHz, $CDCl_3$): δ=2.69 (s, 3H), 5.67 (*exchangeable* s, 1H), 6.89 (d, *J*=8.3 Hz, 1H), 7.11 (d, *J*=8.5 Hz, 1H), 7.31 (dd, *J*=8.5, 2.1 Hz, 1H), 7.46 (d, *J*=2.1 Hz, 1H), 7.70 (d, *J*=8.3 Hz, 1H), 13.08 ppm (*exchangeable* s, 1H); ^{13}C NMR (100 MHz, $CDCl_3$): δ=26.9, 116.1, 119.3, 119.8, 121.0, 121.5, 128.5, 129.6, 129.8, 131.9, 146.6, 151.7, 158.9, 204.1 ppm.

1-(2-Chloro-3,4'-dihydroxy-3'-methyl-[1,1'-biphenyl]-4-yl)ethanone (5o). (86% yield from **5n**) ^{1}H NMR (400 MHz, [D$_6$]acetone): δ=2.26 (s, 3H), 2.73 (s, 3H), 6.93 (d, *J*=8.3 Hz, 1H), 6.98 (d, *J*=8.3 Hz, 1H), 7.18 (dd, *J*=8.2, 2.3 Hz, 1H), 7.25 (d, *J*=1.9 Hz, 1H), 7.94 (d, *J*=8.3 Hz, 1H), 8.53 (*exchangeable* s, 1H), 13.13 ppm (*exchangeable* s, 1H); ^{13}C NMR (100 MHz, [D$_6$]acetone): δ=16.2, 26.9, 115.1, 115.2, 119.7, 121.1, 122.0, 125.0, 128.7, 130.1, 130.6, 132.5, 149.1, 156.7, 159.5 ppm.

Preparation of Final Products 3c-o. General Procedure. A solution of pure ketones **5c-o** (1 eq) in ethanol (6.5 mL/0.34 mmol ketone) was treated with a solution of hydroxylamine hydrochloride (2 eq) in water (1.5 mL/0.68 mmol $NH_2OH{\cdot}HCl$), and the mixture was heated to 50 °C for 16 h. After being cooled to RT, part of the solvent was removed under vacuum, and the mixture was diluted with water and extracted with EtOAc. The organic phase was dried and evaporated to afford a crude residue that was purified by column chromatography (*n*-hexane/EtOAc 9:1 to 7:3 or CH_2Cl_2/MeOH 95:5) to afford the desired ketoxime derivatives.

(*E*)-1-(2-Chloro-4'-fluoro-3-hydroxy-[1,1'-biphenyl]-4-yl)ethanone oxime (3c). White solid; yield 96% from **5c**. ^{1}H NMR (400 MHz, [D$_6$]acetone): δ=2.42 (s, 3H), 6.94 (d, *J*=8.2 Hz, 1H), 7.23 (double AA'XX', $^3J_{HF\text{-}o}$=9.7 Hz, J_{AX}=8.9 Hz, $J_{AA'XX'}$=2.6 Hz, 2H), 7.50 (double AA'XX', $^4J_{HF\text{-}m}$=5.4 Hz, J_{AX}=8.9 Hz, $J_{AA'XX'}$=2.6 Hz, 2H), 7.58 (d, *J*=8.2 Hz, 1H), 10.98 (*exchangeable* s, 1H), 12.46 ppm (*exchangeable* s, 1H); ^{13}C NMR (100 MHz, [D$_6$]acetone): δ=11.0, 115.8 (d, *J*=22.1 Hz, 2C), 120.0, 120.8, 121.6, 126.8, 132.2 (d, *J*=9.1 Hz, 2C), 136.4, 142.3, 155.2, 158.9, 163.3 ppm (d, *J*=245.5 Hz). HPLC analysis: retention time = 26.4 min; peak area, 97 %; HRMS-ESI *m/z* [*M*+H]$^+$ calcd for $C_{14}H_{11}NO_2FCl$: 280.0541, found: 280.0544.

(*E*)-1-(2-chloro-3-hydroxy-4'-(trifluoromethyl)-[1,1'-biphenyl]-4-yl)ethanone oxime (3d). Light-yellow solid; yield 96% from **5d**. ^{1}H NMR (400 MHz, [D$_6$]acetone): δ=2.43 (s, 3H), 6.99 (d, *J*=8.2 Hz, 1H), 7.63 (d, *J*=8.2 Hz, 1H), 7.67-7.71 (m, 2H), 7.81-7.85 (m, 2H), 11.02 (*exchangeable* bs, 1H), 12.51 ppm (*exchangeable* bs, 1H); ^{13}C NMR (100 MHz, [D$_6$]acetone): δ=11.0, 120.5, 120.6, 121.4, 125.4 (q, *J*=271.7 Hz), 125.9 (q, *J*=4.0 Hz, 2C), 127.0, 130.2 (q, *J*=32.2 Hz), 131.0 (2C), 147.8, 144.2, 155.3, 158.8 ppm. HPLC analysis: retention time = 28.6 min; peak area, 95 %; HRMS-ESI *m/z* [*M*+H]$^+$ calcd for $C_{15}H_{11}NO_2F_3Cl$: 330.0509, found: 330.0506.

(*E*)-1-(2-chloro-3,3'-dihydroxy-[1,1'-biphenyl]-4-yl)ethanone oxime (3e). White solid; yield 48% from **5e**. ^{1}H NMR (400 MHz, [D$_6$]acetone): δ=2.41 (s, 3H), 6.86-6.95 (m, 4H), 7.27 (t, *J*=7.8 Hz, 1H), 7.56 (d, *J*=8.3 Hz, 1H), 8.47 (*exchangeable* s, 1H), 10.94 (*exchangeable* s, 1H), 12.42 ppm (*exchangeable* s, 1H); ^{13}C NMR (100 MHz, [D$_6$]acetone): δ=10.9, 115.6, 117.1, 119.7, 120.7, 121.3, 121.5, 126.6, 130.0, 141.6, 143.4, 155.2, 158.0, 158.9 ppm. HPLC analysis: retention time = 20.3 min; peak area, 99 %; HRMS-ESI *m/z* [*M*+H]$^+$ calcd for $C_{14}H_{12}NO_3Cl$: 278.0584, found: 278.0584.

(*E*)-1-(2,3'-dichloro-3,4'-dihydroxy-[1,1'-biphenyl]-4-yl)ethanone oxime (3f). White solid; yield 65% from **5f**. ^{1}H NMR (400 MHz, [D$_6$]acetone): δ=2.40 (s, 3H), 6.92 (d, *J*=8.3 Hz, 1H), 7.10 (d, *J*=8.4 Hz, 1H), 7.27 (dd, *J*=8.4, 2.2 Hz, 1H), 7.44 (d, *J*=2.1 Hz, 1H), 7.55 (d, *J*=8.3 Hz, 1H), 8.99 (*exchangeable* bs, 1H), 10.96 (*exchangeable* bs, 1H), 12.44 ppm (*exchangeable* s, 1H); ^{13}C NMR (100 MHz, [D$_6$]acetone): δ=10.9, 117.2, 119.8, 120.7, 120.7, 121.5, 126.7, 130.0, 131.5, 132.7, 141.8, 153.6, 155.2, 158.9 ppm. HPLC analysis: retention time = 22.5 min; peak area, 99 %; HRMS-ESI *m/z* [*M*+H]$^+$ calcd for $C_{14}H_{11}NO_3Cl_2$: 312.0194, found: 312.0197.

(*E*)-1-(2-chloro-3-hydroxy-4'-(trifluoromethoxy)-[1,1'-biphenyl]-4-yl)ethanone oxime (3g). Light-yellow solid; yield 90% from **5g**. ^{1}H NMR (400 MHz, [D$_6$]acetone): δ=2.42 (s, 3H), 6.97 (d, *J*=8.2 Hz, 1H), 7.41-7.46 (m, 2H), 7.57-7.63 (m, 3H), 12.49 ppm (*exchangeable* bs, 1H); ^{13}C NMR (100 MHz, [D$_6$]acetone): δ=11.0, 120.2, 121.5 (q, *J*=255.6 Hz), 121.5 (2C), 126.9, 129.0, 130.1, 132.1 (2C), 139.3, 141.8, 149.5, 155.2, 158.8 ppm. HPLC analysis: retention time = 29 min; peak area, 78 % (we were unable to improve the purity of this compound, so it was tested as such, without further purification); HRMS-ESI *m/z* [*M*+H]$^+$ calcd for $C_{15}H_{11}NO_3F_3Cl$: 346.0458, found: 346.0457.

(*E*)-1-(2-chloro-3-hydroxy-4'-methoxy-[1,1'-biphenyl]-4-yl)ethanone oxime (3h). Yellow solid; yield 64% from **5h**. ^{1}H NMR (400 MHz, [D$_6$]acetone): δ=2.41 (s, 3H), 3.85 (s, 3H), 6.92 (d, *J*=8.2 Hz, 1H), 7.01 (AA'XX', J_{AX}=8.8 Hz, $J_{AA'XX'}$=2.6 Hz, 2H), 7.40 (AA'XX', J_{AX}=8.9 Hz, $J_{AA'XX'}$=2.6 Hz, 2H), 7.55 (d, *J*=8.3 Hz, 1H), 10.90 (*exchangeable* bs, 1H), 12.40 ppm (*exchangeable* bs, 1H); ^{13}C NMR (100 MHz, [D$_6$]acetone): δ=10.9, 55.6, 114.3 (2C), 119.4, 120.8, 121.6, 126.6, 131.3 (2C), 132.4, 143.1, 155.2, 158.9, 160.4 ppm. HPLC analysis: retention time = 25.6 min; peak area, 96 %; HRMS-ESI *m/z* [*M*+H]$^+$ calcd for $C_{15}H_{14}NO_3Cl$: 292.0740, found: 292.0743.

(*E*)-1-(2-chloro-3-hydroxy-3'-(trifluoromethoxy)-[1,1'-biphenyl]-4-yl)ethanone oxime (3i). White solid; yield 80% from **5i**. ^{1}H NMR (400 MHz, [D$_6$]acetone): δ=2.43 (s, 3H), 6.98 (d, *J*=8.2 Hz, 1H), 7.38-7.43 (m, 2H), 7.49 (dt, *J*=7.8, 1.3 Hz, 1H), 7.62 (t, *J*=7.7 Hz, 1H), 7.63 (d, *J*=8.3 Hz, 1H), 11.03 (*exchangeable* s, 1H), 12.51 ppm (*exchangeable* s, 1H); ^{13}C NMR (100 MHz, [D$_6$]acetone): δ=10.9, 120.4, 120.6, 121.2, 121.4, 121.5 (q, *J*=255.6 Hz), 122.8, 126.9, 129.2, 130.9, 141.5, 142.3, 149.6, 155.3, 158.8 ppm. HPLC analysis: retention time = 28.8 min; peak area, 97 %; HRMS-ESI *m/z* [*M*+H]$^+$ calcd for $C_{15}H_{11}NO_3F_3Cl$: 346.0458, found: 346.0459.

(*E*)-1-(2-chloro-3-hydroxy-3'-methoxy-[1,1'-biphenyl]-4-yl)ethanone oxime (3j). White solid; yield 67% from **5j**. ^{1}H NMR (400 MHz, [D$_6$]acetone): δ=2.42 (s, 3H), 3.84 (s, 3H), 6.94 (d, *J*=8.3 Hz, 1H), 6.96-7.02 (m, 3H), 7.4 (td, *J*=7.7, 1.0 Hz, 1H), 7.57 (d, *J*=8.2 Hz, 1H), 10.93 (*exchangeable* s, 1H), 12.43 ppm (*exchangeable* s, 1H); ^{13}C NMR (100 MHz, [D$_6$]acetone): δ=11.0, 55.6, 114.1, 115.8, 119.8, 120.8, 121.5, 122.4, 126.7, 123.0, 141.6, 143.3, 155.2, 158.9, 160.4 ppm. HPLC analysis: retention time = 25.7 min; peak area, 96%; HRMS-ESI *m/z* [*M*+H]$^+$ calcd for $C_{15}H_{14}NO_3Cl$: 292.0740, found: 292.0745.

(*E*)-2'-chloro-3'-hydroxy-4'-(1-(hydroxyimino)ethyl)-[1,1'-biphenyl]-4-carbonitrile (3k). White solid; yield 71% from **5k**. ^{1}H NMR (400 MHz, [D$_6$]acetone): δ=2.43 (s, 3H), 6.98 (d, *J*=8.2 Hz, 1H), 7.63 (d, *J*=8.3 Hz, 1H), 7.68 (AA'XX', J_{AX}=8.1 Hz, $J_{AA'XX'}$=1.8 Hz, 2H), 7.88 (AA'XX', J_{AX}=8.6 Hz, $J_{AA'XX'}$=1.8 Hz, 2H), 11.04 (*exchangeable* s, 1H), 12.52 ppm (*exchangeable* s, 1H); ^{13}C NMR (100 MHz, [D$_6$]acetone): δ=11.0, 112.4, 199.2, 120.5, 120.7, 121.3, 127.0, 131.2 (2C), 132.8 (2C), 141.5, 144.8, 155.3, 158.8 ppm. HPLC analysis: retention time = 24.4 min; peak area, 96 %; HRMS-ESI *m/z* [*M*+H]$^+$ calcd for $C_{15}H_{11}N_2O_2Cl$: 287.0587, found: 287.0583.

(*E*)-2'-chloro-3'-hydroxy-4'-(1-(hydroxyimino)ethyl)-[1,1'-biphenyl]-3-carbonitrile (3l). Yellow solid; yield 73% from **5l**. ^{1}H NMR (400 MHz, [D$_6$]acetone): δ=2.43 (s, 3H), 7.00 (d, *J*=8.2 Hz, 1H), 7.64 (d, *J*=8.2 Hz, 1H), 7.70 (td, *J*=7.7, 0.6 Hz, 1H), 7.79-7.87 ppm (m, 3H); ^{13}C NMR (100 MHz, [D$_6$]acetone): δ=11.0, 113.2, 119.1, 120.6, 121.4, 127.0, 130.2, 130.5, 132.3, 133.6, 134.8, 141.0, 141.4, 155.3, 158.8 ppm. HPLC analysis: retention time = 24.3 min; peak area, 94 %; HRMS-ESI *m/z* [*M*+H]$^+$ calcd for $C_{15}H_{11}N_2O_2Cl$: 287.0587, found: 287.0591.

(*E*)-1-(2,3'-dichloro-3-hydroxy-4'-methoxy-[1,1'-biphenyl]-4-yl)ethanone oxime (3m). White solid; yield 47% from **5m**. ^{1}H NMR (400 MHz, [D$_6$]acetone): δ=2.42 (s, 3H), 3.97 (s, 3H), 6.95 (d, *J*=8.2 Hz, 1H), 7.21 (d, *J*=8.5 Hz, 1H), 7.40 (dd, *J*=8.5, 2.2 Hz, 1H), 7.49 (d, *J*=2.2 Hz, 1H), 7.58 (d, *J*=8.3 Hz, 1H), 10.96 (*exchangeable* bs, 1H), 12.45 ppm (*exchangeable* bs, 1H); ^{13}C NMR (100 MHz, [D$_6$]acetone): δ=11.0, 56.6, 123.0, 119.9, 120.8, 121.6, 122.3, 126.8, 130.0, 131.6, 133.3, 141.7, 155.2, 155.7, 158.9 ppm. HPLC analysis: retention time = 27.1 min; peak area, 97 %; HRMS-ESI *m/z* [*M*+H]$^+$ calcd for $C_{15}H_{13}NO_3Cl_2$: 326.0351, found: 326.0349.

(*E*)-1-(2-chloro-3-hydroxy-4'-methoxy-3'-methyl-[1,1'-biphenyl]-4-yl)ethanone oxime (3n). White solid; yield 63% from **5n**. ^{1}H NMR (400 MHz, [D$_6$]acetone): δ=2.23 (s, 3H), 2.41 (s, 3H), 3.89 (s, 3H), 6.90 (d, *J*=8.3 Hz, 1H), 6.99 (d, *J*=8.3 Hz, 1H), 7.23-7.25 (m, 1H), 7.26 (dd, *J*=8.3, 2.3 Hz, 1H), 7.54 (d, *J*=8.3 Hz, 1H), 10.91 (*exchangeable* bs, 1H), 12.39 ppm (*exchangeable* bs, 1H); ^{13}C NMR (100 MHz, [D$_6$]acetone): δ=10.9, 16.4, 55.7, 110.4, 119.3, 120.8, 121.7, 126.5, 128.8, 132.1, 132.2, 143.3, 155.2, 158.4, 158.9 ppm. HPLC analysis: retention time = 27.7 min; peak area, 97 %; HRMS-ESI *m/z* [*M*+H]$^+$ calcd for $C_{16}H_{16}NO_3Cl$: 306.0897, found: 306.0901.

(*E*)-1-(2-chloro-3,4'-dihydroxy-3'-methyl-[1,1'-biphenyl]-4-yl)ethanone oxime (3o). Off-white solid; yield 86% from **5o**. ^{1}H NMR (400 MHz, [D$_6$]acetone): δ=2.25 (s, 3H), 2.40 (s, 3H), 6.89 (d, *J*=8.2 Hz, 2H), 7.13 (dd, *J*=8.3, 2.2 Hz, 1H), 7.20 (d, *J*=1.8 Hz, 1H), 7.52 (d, *J*=8.3 Hz, 1H), 8.37 (*exchangeable* s, 1H), 10.88 (*exchangeable* s, 1H), 12.37 ppm (*exchangeable* s, 1H); ^{13}C NMR (100 MHz, [D$_6$]acetone): δ=10.9, 16.2, 115.1, 119.2, 120.8, 121.7, 124.7, 126.5, 128.7, 131.4, 132.6, 143.6, 155.2, 156.1, 158.9 ppm. HPLC analysis: retention time = 21.8 min; peak area, 98 %; HRMS-ESI *m/z* [*M*+H]$^+$ calcd for $C_{15}H_{14}NO_3Cl$: 292.0740, found: 292.0742.

Glucose Uptake Assay. The glucose transport inhibitory activity of the compounds was measured using a radioactive glucose uptake assay as previously described.[13] Briefly, H1299 lung cancer cells grown in 24-well plates were washed twice with serum-free DMEM and incubated with 0.5 mL of the same medium at 37 °C for 2 hr. The cells were washed 3 times with Krebs-Ringer-Hepes (KRP) buffer and incubated with 0.45 mL KRP buffer at 37 °C for 30 min. Compounds were added at a final concentration of 30 µM and incubated for 15 min. Glucose uptake was initiated by the addition of 37 MBq/L 2-deoxy-D-[^{3}H]-glucose and 1 mmol/L regular glucose as final concentrations. After 30 min, glucose uptake was terminated by washing the cells 3 times with cold phosphate buffered saline (PBS). Then cells were lysed with 0.2 M NaOH. The radioactivity retained by the cell lysates was measured by a LS 6000 Series Liquid Scintillation Counter (Beckman Coulter, Inc. Fullerton, CA). IC_{50} values were determined by GraphPad Prism version 6.02 for Windows, GraphPad Software, San Diego California USA, www.graphpad.com.

Proliferation Assay. Cell growth and proliferation was assessed using the MTT proliferation assay kit (Cayman, Ann Arbor, MI) as previously described.[13] Briefly, H1299 lung cancer cells were incubated with or without compounds (30 µM) in cell culture media for 48 hours. Afterward, 10 µL of MTT reagent were added. After additional 3 h of incubation, the culture medium was removed, 100 µL Crystal Dissolving Solution was added to each well, and the absorbance of the solution was measured at 570 nm. Values are reported as the mean ± the standard deviation of three or more independent experiments. Data were analyzed and IC_{50} determined by GraphPad Prism version 6.02 for Windows, GraphPad Software, San Diego California USA, www.graphpad.com.

Relative Binding Affinity Assay. Relative binding affinities were determined by competitive radiometric binding assays with 2 nM [^{3}H]E_2 as tracer, as a modification of methods previously described.[14] The source of ER was purified full-length human ERα and ERβ purchased from Pan Vera/Invitrogen (Carlsbad, CA). Incubations were done at 0 °C for 18-24 h, and hydroxyapatite was used to absorb the purified receptor-ligand complexes (human ERs).[14d] The binding affinities are expressed as relative binding affinity (RBA) values, where the RBA of estradiol is 100%; under these conditions, the K_d of estradiol for ERα is ca. 0.2 nM, and for ERβ 0.5 nM. The determination of these RBA values is reproducible in separate experiments with a CV of 0.3, and the values shown represent the average ± range or SD of 3 or more separate determinations.

Imaging of glucose uptake inhibition using 2-NBDG. A549 cells in RPMI 1640 medium containing 10 % fetal bovine serum (FBS), 1 % penicillin-streptomycin solution were seeded on a 35 mm cover glass bottom dish with 20 mm micro-well cover glass (In Vitro Scientific, Sunnyvale, CA) at a density of 60000 cells/dish. When cells reached 70 % confluence (~16 hour), cells were incubated in the presence or absence of 30 µM Phloretin or ketoximies **3a**,**e**,**f**,**o** in RPMI 1640 medium excluding D-glucose, FBS and phenol red for 30 minutes at 37 °C in a 95 % air/ 5 % CO_2 atmosphere. Then 2-NBDG (50 µM) and Hoechst 33342 (1 µg/mL) were added to the cells. After 15 minutes, the cells were washed with D-glucose, FBS and phenol red free RPMI 1640 medium thrice, and cellular fluorescence was observed using a Zeiss LSM 700 confocal microscope (Zeiss, Oberkochen, Germany). Fluorescence images of 100-120 cells were randomly taken and mean fluorescent intensity of each cells was measured by Image J. The mean fluorescence values were then averaged among four independent experiments.

Molecular modeling. The compounds were built using Maestro 9.0[18] and were subjected to a conformational search (CS) of 1000 steps, using a water environment model (generalized-Born/surface-area model) by means of Macromodel.[19] The algorithm used was based on the Monte Carlo method with the MMFFs force field and a distance-dependent dielectric constant of 1.0. The ligands were then energy minimized using the conjugated gradient (CG) method until a convergence value of 0.05 kcal (mol^{-1} A^{-1}) was reached, using the same force field and parameters used for the CS. The *h*GLUT1 model was extracted from the minimized average structure of the complex between *h*GLUT1 and 13 obtained by us through molecular dynamic simulations.[7] Automated docking was carried out by means of the GOLD 5.1 program.[17] The "allow early termination" option was deactivated, the remaining GOLD default parameters were used, and the ligands were submitted to 30 genetic

algorithm runs by applying the ChemScore fitness function. The best docked conformation was taken into account.

Abbreviations

GLUT1, glucose transporter 1; 2-NBDG, 2-[*N*-(7-nitrobenz-2-oxa-1,3-diazol-4-yl) amino]-2-deoxy-d-glucose; ATP, adenosine triphosphate; PET, positron emission tomography; FDG, 2-[^{18}F]fluoro-2-deoxy-d-glucose; XylE, d-xylose-proton symporter; ER, estrogen receptor; EtOH, ethanol; NMR, nuclear magnetic resonance; ppm, parts per million; NSCLC, non-small cell lung carcinoma; KRP, Krebs-Ringer-Phosphate; PBS, phosphate-buffered saline; Glc, glucose; SAR, structure-activity relationship; MTT, 3-(4,5-dimethylthiazol-2-yl)-2,5-diphenyltetrazolium bromide; RBA, relative binding affinity; RPMI, Roswell Park Memorial Institute; DMSO, dimethyl sulfoxide; H-bond, hydrogen bond; SD, standard deviation; HPLC, high performance liquid chromatography; TLC, thin layer chromatography; LC-MS, liquid chromatography–mass spectrometry; RP, reverse phase; TFA, trifluoroacetic acid; UV, ultraviolet; RT, room temperature; MS, mass spectrometry; ESI, electrospray ionization; HRMS, high-resolution mass spectrometry; s, singlet; d, doublet; dd, double doublet; ddd, double double doublet; t, triplet; q, quartet; m, multiplet; bs, broad signal; IC_{50}, half maximal inhibitory concentration; E_2, estradiol; CV, coefficient of variation; FBS, fetal bovine serum; CS, conformational search; CG, conjugate gradient; MMFF, Merck molecular force field.

Acknowledgements

Support from the National Institutes of Health (R01GM098453 to P.J.H. and F.M.; R01DK015556 to J.A.K.) is gratefully acknowledged. This work was partially supported by Student Enhancement Award (to Y. Qian), Graduate Student Senate Original Work Grant (to Y. Qian), the Donald Clippinger Graduate Fellowship from Ohio University (to Y. Qian).

Keywords: GLUT1 • Warburg effect • cancer metabolism • glycolysis • oximes.

[1] M. G. Vander Heiden, L. C. Cantley, C. B. Thompson, *Science* **2009**, *324*, 1029-1033.

[2] O. Warburg, *Science* **1956**, *123*, 309-314.

[3] L. K. I. Boroughs, R. J. DeBerardinis, *Nat. Cell Biol.* **2015**, *17*, 351-359.

[4] (a) C. Granchi, D. Fancelli, F. Minutolo, *Bioorg. Med. Chem. Lett.* **2014**, *24*, 4915-4925; (b) C. Granchi, F. Minutolo, *ChemMedChem* **2012**, *7*, 1318-1350.

[5] S. J. Bensinger, H. R. Christofk, *Semin. Cell Dev. Biol.* **2012**, *23*, 352-361.

[6] E. C. Calvaresi, P. J. Hergenrother, *Chem. Sci.* **2013**, *4*, 2319-2333.

[7] T. Tuccinardi, C. Granchi, J. Iegre, I. Paterni, S. Bertini, M. Macchia, A. Martinelli, Y. Qian, X. Chen, F. Minutolo, *Bioorg. Med. Chem. Lett.* **2013**, *23*, 6923-6927.

[8] L. Sun, X. Zeng, C. Yan, X. Sun, X. Gong, Y. Rao, N. Yan, *Nature* **2012**, *490*, 361-366.

[9] D. Deng, C. Xu, P. Sun, J. Wu, C. Yan, M. Hu, N. Yan, *Nature* **2014**, *510*, 121-125.

[10] (a) I. Paterni, C. Granchi, J. A. Katzenellenbogen, F. Minutolo, *Steroids* **2014**, *90*, 13-29; (b) F. Minutolo, M. Macchia, B. S. Katzenellenbogen, J. A. Katzenellenbogen, *Med. Res. Rev.* **2011**, *31*, 364-442.

[11] (a) F. Minutolo, S. Bertini, C. Papi, K. E. Carlson, J. A. Katzenellenbogen, M. Macchia, *J. Med. Chem.* **2001**, *44*, 4288-4291; (b) F. Minutolo, M. Antonello, S. Bertini, S. Rapposelli, A. Rossello, S. Sheng, K. E. Carlson, J. A. Katzenellenbogen, M. Macchia, *Bioorg. Med. Chem.* **2003**, *11*, 1247-1257; (c) F. Minutolo, R. Bellini, S. Bertini, I. Carboni, A. Lapucci, L. Pistolesi, G. Prota, S. Rapposelli, F. Solati, T. Tuccinardi, A. Martinelli, F. Stossi, K. E. Carlson, B. S. Katzenellenbogen, J. A. Katzenellenbogen, M. Macchia, *J. Med. Chem.* **2008**, *51*, 1344-1351; (d) F. Minutolo, S. Bertini, C. Granchi, T. Marchitiello, G. Prota, S. Rapposelli, T. Tuccinardi, A. Martinelli, J. R. Gunther, K. E. Carlson, J. A. Katzenellenbogen, M. Macchia, *J. Med. Chem.* **2009**, *52*, 858-867; (e) S. Bertini, A. De Cupertinis, C. Granchi, B. Bargagli, T. Tuccinardi, A. Martinelli, M. Macchia, J. R. Gunther, K. E. Carlson, J. A. Katzenellenbogen, F. Minutolo, *Eur. J. Med. Chem.* **2011**, *46*, 2453-2462.

[12] I. Paterni, S. Bertini, C. Granchi, T. Tuccinardi, M. Macchia, A. Martinelli, I. Caligiuri, G. Toffoli, F. Rizzolio, K. E. Carlson, B. S. Katzenellenbogen, J. A. Katzenellenbogen, F. Minutolo, *J. Med. Chem.* **2015**, *58*, 1184-1194.

[13] Y. Liu, Y. Cao, W. Zhang, S. Bergmeier, Y. Qian, H. Akbar, R. Colvin, J. Ding, L. Tong, S. Wu, J. Hines, X. Chen, *Mol. Cancer Ther.* **2012**, *11*, 1672-1682.

[14] (a) J. A. Katzenellenbogen, H. J. Jr. Johnson, H. N. Myers, *Biochemistry* **1973**, *12*, 4085-4092; (b) K. E. Carlson, I. Choi, A. Gee, B. S. Katzenellenbogen, J. A. Katzenellenbogen, *Biochemistry* **1997**, *36*, 14897-14905.

[15] P. I. Hillerns, Y. Zu, Y. J. Fu, M. Wink, *Z. Naturforsch C* **2005**, *60*, 649-656.

[16] C. Zou, Y. Wang, Z. Shen, *J. Biochem. Biophys. Methods* **2005**, *64*, 207-215.

[17] M. L. Verdonk, J. C. Cole, M. J. Hartshorn, C. W. Murray, R. D. Taylor, *Proteins* **2003**, *52*, 609-623.

[18] *Maestro*, version 9.0 Schrödinger Inc.: Portland, OR, 2009.

[19] *Macromodel*, version 9.7 Schrödinger Inc. Portland, OR, 2009.

Entry for the Table of Contents

FULL PAPER

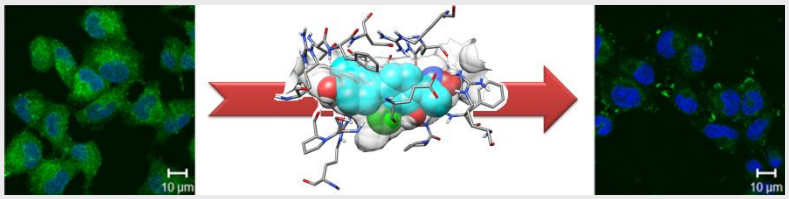

*Carlotta Granchi, Yanrong Qian, Hyang Yeon Lee, Ilaria Paterni, Carolina Pasero, Jessica Iegre, Kathryn E. Carlson, Tiziano Tuccinardi, Xiaozhuo Chen, John A. Katzenellenbogen, Paul J. Hergenrother and Filippo Minutolo**

Page No. – Page No.

Salicylketoximes targeting glucose transporter 1 restrict energy supply to lung cancer cells

Blackout in the city! Enhanced glucose uptake is a consequence of the augmented glycolysis occurring in neoplastic tissues, which warrants a sufficient amount of energy for their rapid growth. New salicylketoxime derivatives are able to “turn the lights off” in cancer cells by blocking their glucose uptake as a consequence of an inhibition of membrane transporter GLUT1.